lets measured in the open sea are very similar, and the size ratio between bubble and droplet spectra is also very similar to that between jet drops and their parent bubbles. Consequently, sea spray appears to be produced mainly by bubble bursting.

At very low wind velocities, spray may be produced by aerodynamic suction at the crests of capillary waves (no actual observation of this has been reported). Accepting this, the number of droplets produced by aerodynamic suction would still be less than the number produced by bubble bursting because there are 10^5 to 10^6 bubbles per cubic meter for the wind velocity range shown in Fig. 2 and relatively few capillary waves on the wind-disturbed water surface (*19*).

At very high wind velocities, water is torn from the wave crests. However, for a limited wind velocity range the bubble concentration increases very rapidly with wind velocity as $U^{4.5}$ (*19*), and for a wide range of velocities the whitecap coverage also increases very rapidly with wind velocity as $U^{3.75}$ (*21*). In other words, although tearing of the water surface occurs at high wind velocities, the bubble concentration, and therefore the concentration of droplets produced by bursting bubbles, also increases very rapidly. Furthermore, the water torn from the wave crest tends to fall back immediately. Thus, bubble bursting appears to be the major mechanism for spray production even at low and high wind velocities.

It is important to identify clearly the mechanisms of spray production in order to estimate quantitatively the effects of spray, especially atmospheric fluxes of metals and organic matter to and from the ocean and material transport from the sea surface. This report should be helpful in establishing the relative importance of bubbles for transporting sea salts and pollutants to air and land.

JIN WU

College of Marine Studies, University of Delaware, Newark 19711

References and Notes

1. A. H. Woodcock, *J. Meterol.* **9**, 200 (1952).
2. _____ and D. C. Blanchard, *Tellus* 7, 437 (1955).
3. Jin Wu, *J. Geophys. Res.* **78**, 511 (1973).
4. _____, *ibid.* **79**, 4107 (1974).
5. R. A. Duce and E. J. Hoffman, *Annu. Rev. Earth Planet. Sci.* **4**, 187 (1976).
6. E. R. Baylor, M. B. Baylor, D. C. Blanchard, L. D. Syzdek, C. Appel, *Science* **198**, 575 (1977).
7. D. C. Blanchard, *Pure Appl. Geophys.* **116**, 302 (1978).
8. G. R. Valenzuela, M. B. Liang, J. C. Daley, *J. Mar. Res.* **29**, 69 (1971).
9. D. C. Blanchard and A. H. Woodcock, *Ann. N.Y. Acad. Sci.* **338**, 330 (1980).
10. D. C. Blanchard, *Prog. Oceanogr.* **1**, 71 (1963).
11. J. A. Day, *Q. J. R. Meteorol. Soc.* **90**, 72 (1964).
12. F. MacIntyre, *J. Geophys. Res.* **77**, 5211 (1972).
13. Jin Wu, *ibid.* **84**, 1693 (1979).
14. B. J. Mason, *Nature (London)* **174**, 470 (1954).
15. D. C. Blanchard and A. H. Woodcock, *Tellus* **9**, 145 (1957).
16. S. Hayami and Y. Toba, *J. Oceanogr. Soc. Jpn.* **14**, 145 (1958).
17. D. A. Kolovayev, *Oceanology* **15**, 659 (1976).
18. B. D. Johnson and R. C. Cooke, *J. Geophys. Res.* **85**, 3761 (1979).
19. Jin Wu, *ibid.*, in press.
20. J. Yu. Preobrazhenskii, *Fluid Mech. Sov. Res.* **2**, 95 (1973).
21. Jin Wu, *J. Phys. Oceanogr.* **7**, 1064 (1979).
22. Supported by Physical Oceanography Program, National Science Foundation, under grant OCE 77-26508.

3 November 1980; revised 16 January 1981

Threads in the Hagfish Slime Gland Thread Cells: Organization, Biochemical Features, and Length

Abstract. *Scanning electron microscopy in conjunction with cell isolation procedures revealed details of the packing of threads in hagfish slime gland thread cells. Biochemical studies indicate that the thread is largely composed of a protein subunit with a molecular weight of 63,500. Mathematical calculations suggest that the thread may attain lengths of 60 centimeters or more.*

The epidermis and epidermally derived slime glands of hagfishes, perhaps the most primitive living vertebrates, produce copious quantities of mucus (*1*). Hagfish mucus (*2*) and mucus-producing tissues (*3–7*) have been described by various investigators. Although the cells of the epidermis proper contribute some mucus to the total secreted by the hagfish, the bulk of the mucus is formed by cells released from highly specialized slime glands. The encapsulated slime glands (Fig. 1A) are connected to the epidermal surface by a small pore; a single row of pores runs lengthwise along the ventrolateral body wall of each side of the animal. The glands are filled with two types of large secretory cells (Fig. 1, A and B): gland mucous cells and gland thread cells. When these cells are discharged through the pore into the surrounding seawater they break (holocrine secretion). The contents of the broken gland mucous cells interact with seawater to form a thick, clear mucus; the gland thread cells, upon breaking, release long fibrous threads that uncoil and become embedded in the mucus, thus increasing the overall viscosity of the mucus. The gland thread cell appears to be highly specialized (*4–7*), but its internal organization has not been elucidated. We now describe the internal organization of the cell's thread and its biochemical composition and offer a mathematical basis for estimating its length (*8*).

Large quantities of isolated gland thread cells are prepared for scanning electron microscopy by a modification of Ferry's electrical stimulation technique (*4*). Briefly, Pacific hagfish (*Eptatretus stoutii*) anesthetized in MS-222 (ethyl *m*-aminobenzoate methanesulfonate) are removed from seawater, draped over a beaker, and blotted dry. A mild electrical shock administered to the skin adjacent to a slime gland pore causes a localized contraction of skeletal muscle cells that surround the capsule of the slime gland. This contraction squeezes both the gland thread and gland mucous cells through the pore of the slime gland onto the epidermal surface where they are harvested with a spatula and immersed in fixative (3 percent formaldehyde and 3 percent glutaraldehyde in 0.1*M* sodium cacodylate, *p*H 7.3). The gland thread cells, which do not uncoil when handled in this manner, are separated from the gland mucous cells, which break under this condition, by mild centrifugation. The thread cells are then washed, rendered conductive by the osmium-thiohydrocarbazide-osmium technique (*9*), dehydrated, and critical-point dried; alternatively, the washed gland thread cells are dehydrated, critical-point dried, and rendered conductive by sputter-coating. Cells prepared either way look similar when viewed with the scanning electron microscope, and loss of the gland thread cell membrane, as frequently occurs, permits direct visualization of the thread.

A mature gland thread cell (Fig. 1C) is roughly ellipsoidal in shape with one end slightly blunted and the other slightly pointed. At the cell periphery the individual thread strands lie adjacent to one another and appear to form a circumferentially oriented, helically wound cable (Fig. 1, C and D). We refer to this peripheral appearance of the thread as the cabling effect since the thread does not form a true cable. The cabling effect is pronounced at the blunt end and middle portion of the cell but becomes less distinct at the pointed end (Fig. 1, C and D). Since many isolated gland thread cells separate, pull apart, or loosen up during preparation for scanning electron microscopy (Fig. 1, E, F, and G), direct visualization of the packing of the thread

0036-8075/81/0417-0326$00.50/0

is possible. We observed that, as the thread turns inward (Fig. 1, E, F, and G), the cabling effect disappears; the single-stranded thread forms a loop, which is repeated hundreds of times. One end of each loop is directed toward the pointed end of the cell and at the same time toward an imaginary central axis passing lengthwise through the cell; the other end of each loop is directed at once toward the blunt end of the cell and the cell periphery (Fig. 1, E, F, and G). The association and overlapping of adjacent portions of the loop components at the cell periphery result in the cabling effect illusion (Fig. 1, E, F, and G). These hundreds of adjacent, sequential, and continuous loops form a series of conical groupings of loops, each of which is inserted into the conical grouping above it (that is, the one toward the pointed end) and caps the conical grouping below it (that is, the one toward the blunt end) (Fig. 1, E and G). A slight pitch to each conical grouping results in the overall helical pattern observed at the blunt end and middle portion of the cell and accounts for the fact that each conical grouping is in fact continuous with the conical grouping above and below it (Fig. 1, C, E, and G). Because of this packing arrangement, a single intact thread can unwind without becoming tangled when an isolated cell breaks (Fig. 1, E, F, and G).

For biochemical studies, electrically obtained gland mucous and gland thread cells are broken by immersion in seawater, and the threads are cleared of the viscous material by twisting them onto glass stirring rods. The tightly wound threads are then scraped off the ends of the stirring rods, washed fully in distilled water, then repeatedly washed in increasing and decreasing concentrations of mixtures of ethanol and water, and the final washings are in distilled water. The purified threads are solubilized in 10 percent sodium dodecyl sulfate (SDS) and 1 percent β-mercaptoethanol; SDS–polyacrylamide gel electrophoresis of the isolated, solubilized threads (Fig. 2) indicates a principal protein subunit with a molecular weight of approximately 63,500 and possibly a slightly heavier component between 64,500 and 65,000 daltons (*10*).

The length of individual threads has not been measured accurately, though estimates of a few centimeters have been made (*4*, *5*). We suggest a mathematical procedure for estimating the approximate length of the thread. Assumptions must be made about (i) cell shape, (ii) thread geometry, and (iii) the percent of the cell volume occupied by the thread.

With respect to shape, the cell was assumed to be an ellipsoid having axes of length $2a$, $2b$, and $2b$.

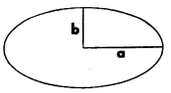

The volume of such an ellipsoid can be calculated from

$$V_e = \frac{4}{3}\pi ab^2 \quad (1)$$

To calculate the length of the thread, we assumed that the thread was cylindrical in shape with a uniform diameter d.

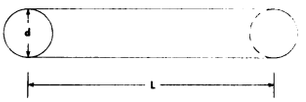

The volume of the thread V_t in this case would be expressed as

$$V_t = \frac{\pi d^2}{4} L \quad (2)$$

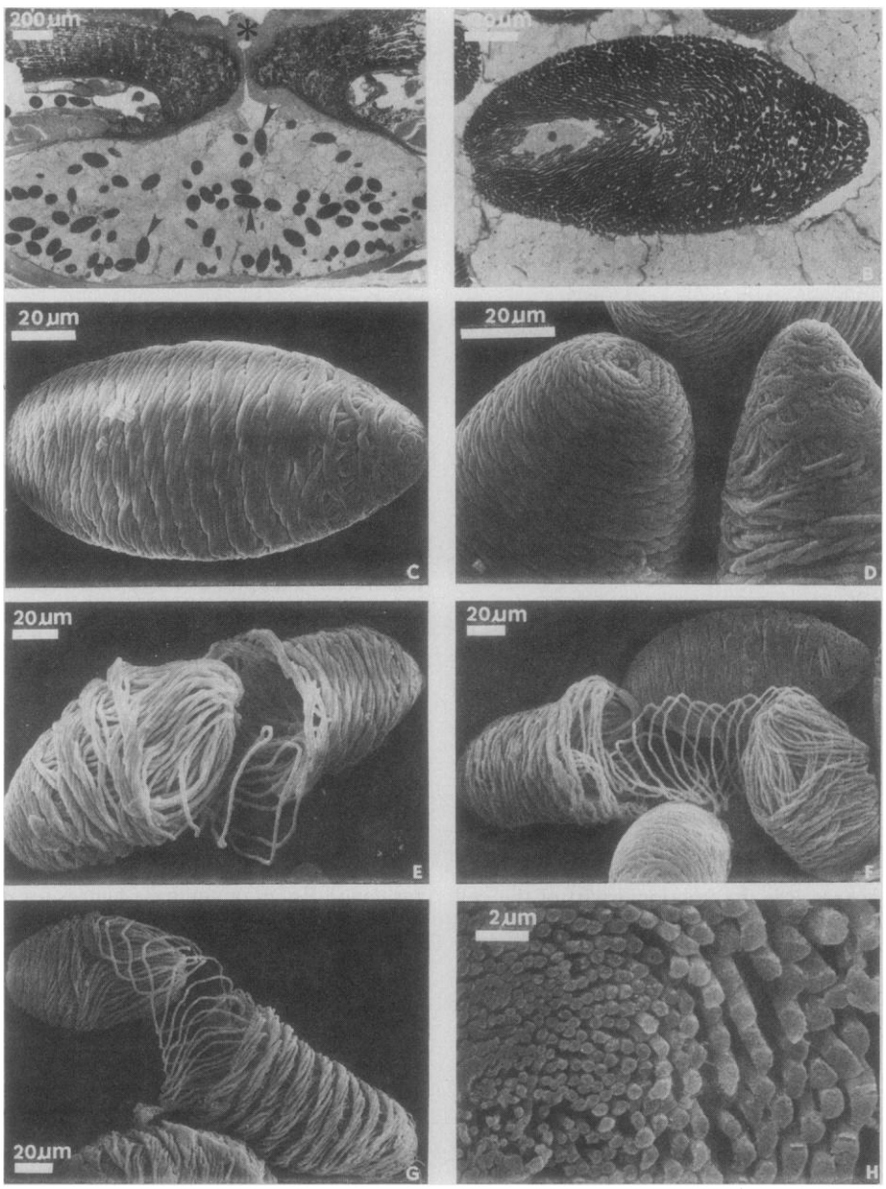

Fig. 1. (A) Cross section (1 µm thick) through a slime gland embedded in Epon. The pore is marked by the asterisk (*). Some dark-staining thread cells are indicated by arrows (▶); mucous cells are light stained. The gland is surrounded by a thin connective tissue capsule and skeletal muscle cells. (B) A cross section (1 µm thick) through the longitudinal axis of a thread cell revealing the nucleus, nucleolus, and a cytoplasm filled largely with thread profiles. (C to F) Scanning electron micrographs of hagfish thread cells. (C) An isolated thread cell revealing its overall ellipsoid shape with one end slightly blunted and the other end slightly pointed. The thread appears to be arranged into a cable, particularly at the blunt and middle portions of the cell. (D) Portions of two adjacent thread cells showing the blunt end of one cell on the left and the more pointed end of an adjacent cell on the right. (E to G) Thread cells that have been pulled apart or have loosened up reveal that the surface cabling effect is an illusion and that, as the thread turns inward and toward the pointed end, the cabling effect is lost. (H) A thread cell cut open with a razor blade reveals the tapered nature of the thread.

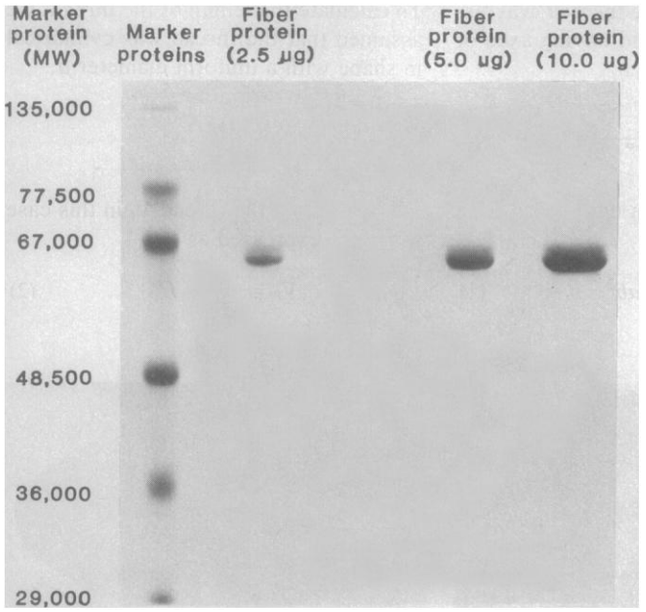

Fig. 2. The SDS–polyacrylamide gel electrophoresis of thread protein showing six marker proteins and three thread proteins solubilized in 10 percent SDS and 1.0 percent β-mercaptoethanol. The thread appears to be comprised primarily of a protein subunit with a molecular weight (*MW*) of 63,500; there may also be a minor second subunit with a molecular weight of 64,500 to 65,000.

where L is the length of a cylindrical thread. In reality, the thread is not cylindrical, but tapered (Fig. 1, B and H). In this case we assumed the fiber to be uniformly tapered along its length, with end diameters d and e

and with

$$V_t = \frac{\pi L_t}{12}(d^2 + de + e^2) \quad (3)$$

where L_t is the length of the tapered thread. Alternatively, V_t may be expressed as

$$V_t = PV_e \quad (4)$$

where P is the fractional part of the cell volume occupied by the thread. Substituting for V_e of Eq. 1 in Eq. 4, we get

$$V_t = P\frac{4}{3}\pi ab^2 \quad (5)$$

By setting Eqs. 2 and 5 equal to each other and solving for L, we arrive at a formula for calculating the length of a thread with uniform diameter

$$L = \frac{16}{3}P\frac{ab^2}{d^2} \quad (6)$$

If we set Eqs. 3 and 5 equal to each other, we can solve for L_t

$$L_t = 16P\frac{ab^2}{(d^2 + de + e^2)} \quad (7)$$

For example, if we assume that (i) the thread cell is an ellipsoid (a = 63.3 μm and b = 31.7 μm), (ii) the thread is not tapered (d = 1 μm), and (iii) 70 percent of the cell volume is occupied by thread (P = 0.7), then the length L of the thread in the thread cell in Fig. 3 is 23.7 cm by Eq. 6.

If we use Eq. 7 and assume that d = 0.5 μm and e = 1.5 μm, then L_t = 21.9 cm. Thus, even though the fiber is tapered, a fairly accurate estimate of its length can be made from Eq. 6 if we have a good average diameter of the thread. Even P is not terribly critical for an approximate calculation. If P is 0.6 or 0.8, instead of 0.7, an error of 1/7 or 15 percent is introduced into the calculation of L. On the other hand, the formula is more sensitive to error in d; if d is off by a factor of 2, L is off by a factor of 4. Therefore, to get an accurate estimate of the thread length it is crucial to work with an accurate average diameter d with Eq. 6, or accurate figures for d and e with Eq. 7. From these calculations, we estimate that large gland thread cells may contain threads approaching 60 cm in length.

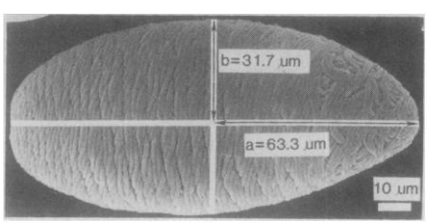

Fig. 3. Scanning electron micrograph of isolated average-sized thread cell. The length of the thread in this cell was estimated to be L = 23.7 cm (assuming an untapered thread with diameter d = 1 μm) or L_t = 21.9 cm (assuming a tapered thread with end diameters d = 0.5 and e = 1.5 μm). See text for explanation of thread length calculations and assumptions.

Highly specialized cells often provide opportunities to study problems related to cell differentiation. The large hagfish slime gland thread cell, which is programmed to do a very specific thing —manufacture and pack a long and continuous protein cytoplasmic thread capable of unwinding to lengths of perhaps 60 cm or more—may provide a model for studying problems related to protein subunit synthesis and assembly, intracellular packing of cellular products, interactions of fibrous proteins with other secretory cell products, and establishment of in vitro protein-synthesizing systems capable of generating macromolecular fibrous polymers.

STEPHEN W. DOWNING
Department of Biomedical Anatomy, University of Minnesota School of Medicine, Duluth 55812
ROBERT H. SPITZER
Department of Biochemistry, Chicago Medical School, North Chicago, Illinois 60664
WILMAR L. SALO
Department of Biochemistry, University of Minnesota School of Medicine
J. SCOTT DOWNING
Department of Mathematics and Computer Science, University of Nebraska, Omaha 68182
LEO J. SAIDEL
ELIZABETH A. KOCH
Department of Biochemistry, Chicago Medical School

References and Notes

1. R. Strahan, *Copeia* **2**, 165 (1959).
2. A. Lehtonen, J. Kärkkäninen, E. Haati, *Acta Chem. Scand.* **20**, 1456 (1966); N. Seno, F. Okiyama, K. Anno, *Biochim. Biophys. Acta* **264**, 229 (1972); R. H. Spitzer, S. W. Downing, E. A. Koch, M. A. Kaplan, *Comp. Biochem. Physiol.* **54B**, 409 (1976).
3. W. J. W. Fan, *Anat. Rec.* **151**, 348 (1965); T. J. Leppi, *Am. Zool.* **6**, 580 (1966); *Anat. Rec.* **157**, 278 (1967); *Histochemie* **15**, 68 (1968); S. W. Downing and S. I. Roth, *Anat. Rec.* **175**, 309 (1973); S. W. Downing, R. H. Spitzer, M. A. Kaplan, O. H. Callaghan, E. A. Koch, C. Locke, *Fed. Proc. Fed. Am. Soc. Exp. Biol.* **36**, 1239 (1977); S. W. Downing and R. H. Spitzer, *Anat. Rec.* **193**, 526 (1979); R. H. Spitzer, S. W. Downing, E. A. Koch, *Cell Tissue Res.* **197**, 235 (1979).
4. J. D. Ferry, *J. Biol Chem.* **138**, 263 (1941).
5. W. W. Newby, *J. Morphol.* **78**, 397 (1946).
6. T. Blackstad, in *The Biology of Myxine*, A. Brodal and R. Fänge, Eds. (Universitetsforlaget, Oslo, 1963), pp. 195–230.
7. K. Terakado, M. Ogawa, Y. Hashimoto, H. Matsuzaki, *Cell Tissue Res.* **159**, 311 (1975).
8. Some of these observations were reported at the 93rd Annual Session of the American Association of Anatomists, Omaha, Nebr., 30 April 1980.
9. R. O. Kelley, R. A. Dekker, J. G. Bluemink, *J. Ultrastruct. Res.* **45**, 254 (1973).
10. These results disagree with those of Hashimoto *et al.* [as cited in (*7*)] who reported that the threads were comprised of fibrous protein or proteins with a molecular weight or molecular weights in the 14,000 to 18,000 range.
11. We thank M. J. Kuhlmey for aid in preparing the manuscript. Supported by National Science Foundation grant PCM-8011775, University of Minnesota Graduate School grant-in-aid of research 419-0325-4909-02 to S.W.D., and a grant from the Asthmatic Children's Aid to R.H.S.

12 June 1980; revised 17 October 1980